Quasi-elastic neutron scattering studies on bacterial spores and their hydration water

Alexandre Colas de la Noue, Tatsuhito Matsuo, Francesca Natali, Michael M Koza, Tilo Seydel, Fatima Fekraoui, Jean-Marie Perrier-Cornet, Judith Peters

▶ **To cite this version:**

Alexandre Colas de la Noue, Tatsuhito Matsuo, Francesca Natali, Michael M Koza, Tilo Seydel, et al.. Quasi-elastic neutron scattering studies on bacterial spores and their hydration water. Scientific Reports, 2026, pp.1-39. ⟨10.1038/s41598-026-44676-1⟩. ⟨hal-05575529⟩

HAL Id: hal-05575529

https://hal.inrae.fr/hal-05575529v1

Submitted on 1 Apr 2026

HAL is a multi-disciplinary open access archive for the deposit and dissemination of scientific research documents, whether they are published or not. The documents may come from teaching and research institutions in France or abroad, or from public or private research centers.

L'archive ouverte pluridisciplinaire **HAL**, est destinée au dépôt et à la diffusion de documents scientifiques de niveau recherche, publiés ou non, émanant des établissements d'enseignement et de recherche français ou étrangers, des laboratoires publics ou privés.

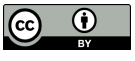

Distributed under a Creative Commons CC BY 4.0 - Attribution - International License

Scientific Reports

https://doi.org/10.1038/s41598-026-44676-1

Article in Press

Quasi-elastic neutron scattering studies on bacterial spores and their hydration water

Received: 3 June 2025

Accepted: 12 March 2026

Published online: 21 March 2026

Cite this article as: Colas de la Noue A., Matsuo T., Natali F. *et al.* Quasi-elastic neutron scattering studies on bacterial spores and their hydration water. *Sci Rep* (2026). https://doi.org/10.1038/s41598-026-44676-1

Alexandre Colas de la Noue, Tatsuhito Matsuo, Francesca Natali, Michael M. Koza, Tilo Seydel, Fatima Fekraoui, Jean-Marie Perrier-Cornet & Judith Peters

We are providing an unedited version of this manuscript to give early access to its findings. Before final publication, the manuscript will undergo further editing. Please note there may be errors present which affect the content, and all legal disclaimers apply.

If this paper is publishing under a Transparent Peer Review model then Peer Review reports will publish with the final article.

ARTICLE IN PRESS

© The Author(s) 2026. **Open Access** This article is licensed under a Creative Commons Attribution-NonCommercial-NoDerivatives 4.0 International License, which permits any non-commercial use, sharing, distribution and reproduction in any medium or format, as long as you give appropriate credit to the original author(s) and the source, provide a link to the Creative Commons licence, and indicate if you modified the licensed material. You do not have permission under this licence to share adapted material derived from this article or parts of it. The images or other third party material in this article are included in the article's Creative Commons licence, unless indicated otherwise in a credit line to the material. If material is not included in the article's Creative Commons licence and your intended use is not permitted by statutory regulation or exceeds the permitted use, you will need to obtain permission directly from the copyright holder. To view a copy of this licence, visit http://creativecommons.org/licenses/by-nc-nd/4.0/.

ARTICLE IN PRESS

Quasi-elastic neutron scattering studies on bacterial spores and their hydration water

Alexandre COLAS de la NOUE [1,2,†], Tatsuhito Matsuo[3,4,5,†], Francesca NATALI[6], Michael M. Koza[4], Tilo Seydel[4], Fatima Fekraoui[7], Jean-Marie PERRIER-CORNET[1], Judith PETERS[4,5,8,*]

[1]*Bourgogne Europe, Institut Agro, INRAE, UMR PAM, 1 esplanade Erasme, F-21000 Dijon, France*

[2]*Qualisud, Univ Montpellier, CIRAD, Montpellier SupAgro, Univ d'Avignon, Univ de la Réunion, Montpellier, France*

[3]*Department of Health and Medical Sciences, Hiroshima International University, Hiroshima, Japan*

[4]*Institut Laue-Langevin, 71 avenue des Martyrs, CS 20156, 38042 Grenoble Cedex 9, France*

[5]*Univ. Grenoble Alpes, CNRS, LiPhy, 38000 Grenoble, France*

[6]*CNR-IOM & INSIDE@ILL c/o Operative Group in Grenoble (OGG) F-38042 Grenoble, France*

[7]*UMR 0545 Fromage, INRAE Aurillac, 15000 AURILLAC, France*

[8]*Institut Universitaire de France, France*

† These authors contributed equally.

*For correspondence. E-mail : jpeters@ill.fr

ARTICLE IN PRESS

ARTICLE IN PRESS

Abstract

Spores are bacteria passed into a metabolically dormant state due to starvation and awaiting better external conditions to germinate and colonize the medium again. Their resistance to numerous stress factors is amazing and the reasons behind are still not completely unveiled. Water seems to play an important role for that, as hydration inside the spores is reduced but paired with a remarkable water mobility. To learn more about these facts, we applied a sophisticated approach: we first analysed neutron scattering spectra of whole spores, then we subtracted spectra corresponding to proteins, lipids and sugars to obtain results as close as possible to the water signal. Our procedure revealed strongly reduced rotational dynamics of the proteome, but a high mobility of water molecules and small molecular subgroups at the sub-nanosecond time scale. Such combination might be key to explain the dormant state of spores which is vigilant to revive in adapted conditions.

ARTICLE IN PRESS

ARTICLE IN PRESS

Introduction

Sporulation is a protective mechanism of gram-positive bacteria permitting them to survive in harsh conditions. When nutrients are lacking, some bacteria are able to sporulate and thus become metabolically inactive, germinating in presence of germinants or with specific physical conditions (pressure, abrasion). Bacterial spores have not yet completely unveiled the secret of their amazing resistance to external stress factors including light and ionizing radiation, wet and dry heat, vacuum, chemicals, enzymes, high hydrostatic pressure and mechanical disruption [1,2]. Some reasons are certainly related to biochemistry as chemical detoxification or DNA reparation tools, but biophysical properties are as important, for instance concerning structural and dynamical properties of the various components. Much more than cells, the spores have a multi-layered structure and thus efficient boundaries between the spore and its environment, but also between different compartments. An endospore like *Bacillus subtilis*, which is studied in the following in its wild-type (WT) and mutant form, has an outer crust surrounding a coat, both are protein-based. The next inner layer is the cortex, a peptidoglycan layer which is surrounded by an outer and inner plasma membrane. In the center is situated the spore's core containing DNA, RNA and most soluble proteins. DNA is protected by chaperone proteins called small acid soluble spore proteins (SASPs) (see figure 1). In contrast to growing cells, 80% (i.e. 80 g per 100 g of wet weight) or more water [3], the core has a reduced water content between 20 and 40 % [1,4], but a high concentration of dipicolinic acid (DPA) mostly

ARTICLE IN PRESS

complexed by ions (generally Ca^{2+} and Mn^{2+}). The inner membrane (IM) contains phospholipids and fatty acids like the plasma membrane of a growing cell. This membrane is naturally compacted what makes it rather impermeable to small molecules, except water. The cortex is formed by a thick peptidoglycan layer (about 29% in mass) with □-lactam muramic residues not reticulated. Beneath the cortex is a small envelope that becomes the cell wall as the spore germinates. The role of the outer membrane has not yet been clearly identified. The coat is composed by a rather rigid protein structure with a relatively low permeability to external molecules. One possible strategy to investigate the functionalities of the different layers is the use of mutants lacking specific parts of the spore structure (see Materials and Methods).

ARTICLE IN PRESS

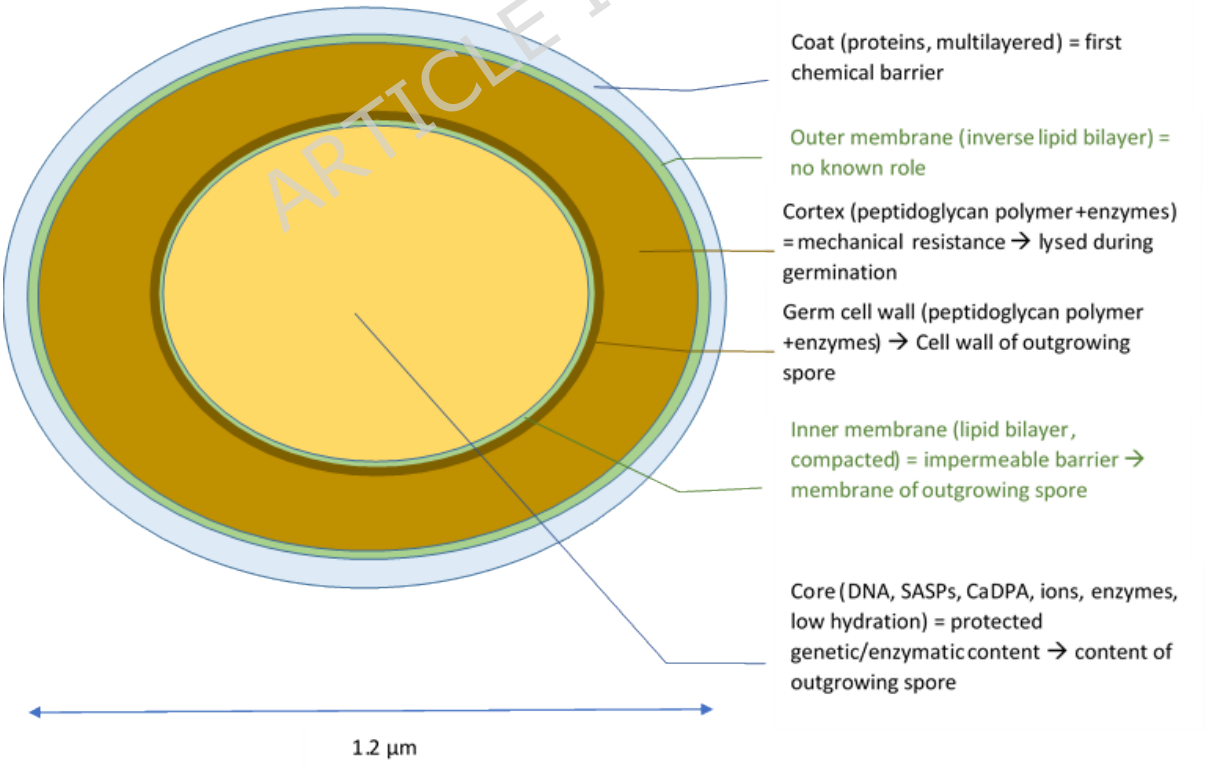

ARTICLE IN PRESS

Figure 1: Schematic representation of the multilayered structure, composition and functionality of a *Bacillus subtilis* spore.

The role of water in the spore's resistance against several stress factors was long time debated as spores are less hydrated than growing cells what could contribute to slow down the protein motions, to compact the structure and likely to better resist to stress. In a seminal work, Sunde et al. [5] and Friedline et al. [6] shed light on the physical state of water in bacterial spores by means of NMR experiments. The various regions of a spore have significantly different water contents, which can be estimated by 20 – 40 % in the core and 40 – 60 % in the non-core parts (cortex and coat) [5]. Such distribution can at least be partly explained by the low permeability of the inner membrane, even though water exchange remains possible within the time scale of ms – s.

The low water content of the core is at the origin of speculations about a glassy state in the core [7], but this view was challenged [8] as the rotational correlation time of the water molecules in the core was similar to that of proteins hydrated at a level of 0.6 g H_2O per gram of dry proteins, usually denoted by h [5]. It was shown that a hydration level of $h = 0.4$ corresponds indeed to about one water layer at the protein surface and is sufficient to guarantee full functionality [9,10]. The state inside the core is therefore fully comparable to the situation of hydrated protein powders, which can be used at sub-zero temperatures, as they are not prone to ice and thus Bragg peak formation. Such proteins are capable of undergoing the dynamical transition around 220 K [11], which was interpreted as an onset

ARTICLE IN PRESS

of anharmonic motions mandatory for functionality [12]. Even in such environment, rotational diffusional motions of proteins are possible albeit they might be slowed down considerably.

Another important aspect is the confinement of proteins in a very limited space. For the sake of a better access to information on a particular protein type, many biochemical studies are carried out in diluted solutions of this sole protein. However, such a state is far from the reality of existence of most of the proteins within cells and newer investigations underline the role of the environment which contributes to the stabilization of the biomolecular systems, to the excluded volume effect, and the modulation of molecular dynamics [13-16]. Confinement can have a protective effect against external conditions, avoiding for instance protein's aggregation at high temperature rendering the denaturation reversible [17] or immobilizing a protein under high hydrostatic pressure.

Direct measurements of water content and dynamics inside of bacterial spores are difficult as most experimental techniques do not permit to differentiate the water populations in the various compartments. Sunde et al. demonstrated in an impressive way to which extent NMR gives access to quantitative results and estimations of several quantities including notably information on long-time rotational dynamics by its inherent access to angular correlations [5]. Another possibility is the use of incoherent neutron scattering, which probes the ensemble-averaged single-particle self-dynamics and is mainly sensitive to the signal of hydrogen atoms due to their high incoherent scattering cross section [18]. In addition, quasi-elastic neutron scattering probes the dependence of the

ARTICLE IN PRESS

scattering signal arising from diffusive dynamics in the sample on the energy and momentum transfer from and to the neutron, which are the complementary variables of time and amplitudes, respectively. From here, it is possible to separate various motions according to their relaxation times and spatial extensions [19]. In the following, we present such an approach providing dynamical characteristics of the bacterial spores and the water inside and surrounding *Bacillus subtilis*.

Materials and Methods

Strains

In the present study, we used the *Bacillus subtilis* WT strain PS533 derived from the strain 168 and the mutant FB122 (ΔsleB::spc ΔspoVF::tet) , which lacks most part of DPA in the core and also sleB enzyme [20]. We had moreover chemically decoated strains of these two versions of spores, e.g. with or without the coat.

Spore production

All spore preparations were produced at 37°C for 48 to 72h in 2*SG liquid medium as described previously [21] before harvesting. Spore suspensions were washed at least 10 times with cold distilled water prior to use, stored for at least one week at 4°C and washed again several times. All spore preparations were exempt of spore debris and germinated cells and purity was higher than 98% as observed by phase-contrast microscopy (cf. Figure 2). The spores were recovered by centrifugation at 10000g - 5 min to pellet cells and prepared for neutron experiments as explained hereafter.

ARTICLE IN PRESS

Decoated spores were prepared according to a procedure described in [22]. Spores were suspended at an OD600 nm of ca. 10–15 for 30 min at 70 °C in 1% sodium dodecyl sulfate (SDS), 0.1 M NaOH, 0.1 M NaCl and 0.1 M dithiothreitol in order to extract coat proteins. The decoated spores were washed extensively with distilled water (ca. 8 times) and stored at 4 °C in PBS. The decoating efficiency was checked by following the decrease in OD600 nm in the presence of 0.5 mg/ml of lysozyme.

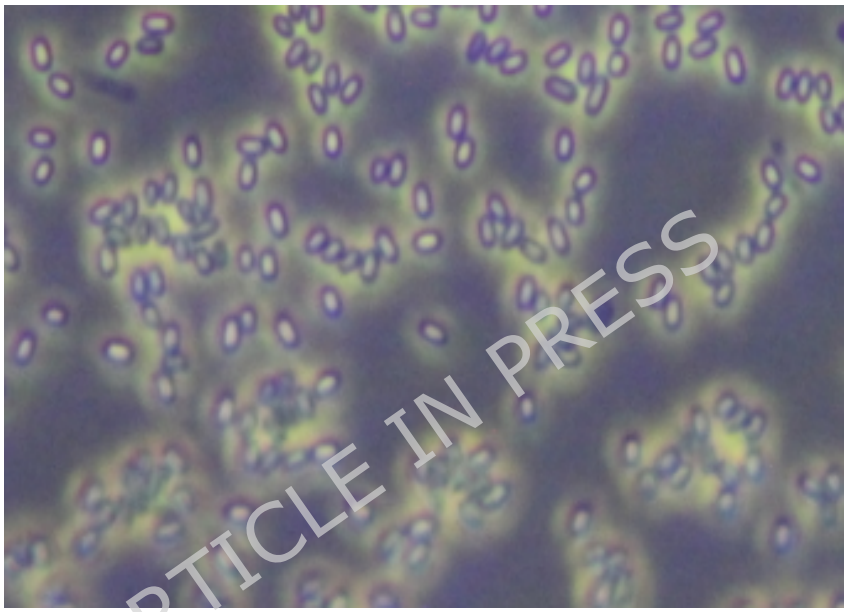
ARTICLE IN PRESS

Figure 2 : Example of microscopic image of *Bacillus subtilis* spores using phase contrast objective (x100) after growing, sporulation and washing stages. “Bright spore” are dormant spores.

Spore preparation for neutron experiments

Spore samples were prepared in H_2O 1 mM phosphate buffer at pH 8 (not corrected for isotope effects). Sample thickness was 0.4 mm to avoid too much absorption and multiple scattering. We wanted to apply here a

ARTICLE IN PRESS

similar approach as Tehei et al. [23] to shed light specifically on bound and free water populations within the samples, which are particularly visible when measuring in H_2O. Indeed, the incoherent scattering cross section is at least 40 times higher for hydrogen than for any other atom occurring in biological systems [18] what permits to highlight certain parts of our samples. Six different samples were chosen for the investigations: PS533 and FB122 as intact and decoated spores in fully hydrated form samples (> 1g H_2O/g sample) and two intact samples of PS533 and FB122 at 75 % relative humidity (equilibrated over 75% water atmosphere). Throughout this paper, the latter samples are called “dried” samples against the fully hydrated samples. The samples for the different instruments were freshly prepared and checked for their weight before and after the experiment to insure no water loss.

ARTICLE IN PRESS

Elastic and Quasi-elastic neutron scattering measurements on IN13, IN16B and IN6

Elastic incoherent neutron scattering (EINS) experiments were executed on the thermal backscattering spectrometer IN13 [24] (ILL, Grenoble, France), which has an energy resolution of 8 μeV and a momentum transfer range $0.2 < Q < 4.9$ Å^{-1} between the incoming and scattered neutron, corresponding to a timescale of about 100 ps. Here localized motions can be monitored. Quasi-elastic neutron scattering (QENS) experiments were performed as a function of temperature on the high flux backscattering spectrometer IN16B [25] (ILL, Grenoble, France), characterized by a momentum transfer range $0.1 < Q < 1.8$ Å^{-1} with a very

ARTICLE IN PRESS

good energy resolution of 0.75 eV. The instrument gives thus access to the timescale of about 1 ns permitting to observe diffusional motions and dynamics of the entire spore or within its components. We further used the cold neutron time-of-flight spectrometer IN6 at ILL, which monitors short times up to 20 ps including fast local motions of small molecules like water or movements of functional groups such as the rotation of hydrogen atoms around carbon in a methyl group. The covered Q-range is here about 0.3 – 2 $Å^{-1}$. The ILL data is available at 10.5291/ILL-DATA.8-04-686 [26].

Data were first reduced by subtracting scattering from the empty sample holder, then normalized to a vanadium spectrum providing the relative detector efficiency and the instrumental resolution. Absorption correction was based on the correction formula of Paalman–Pings [27]. The complete data reduction was carried out using the LAMP software [28].

The sample mass and thickness were suitably chosen to optimize the compromise between good signal-to-noise ratio and minimum multiple scattering contribution. For this purpose, a transmission around 90 % was kept for all samples.

The elastic incoherent intensity is given within the Gaussian approximation [29] by the static structure factor at zero energy exchange ω

$$S(Q,\omega \approx 0) \sim e^{-\frac{1}{6}\langle u^2\rangle Q^2}, \quad (1)$$

where $\langle u^2 \rangle$ is the average atomic mean square displacement (MSD). This Gaussian approximation supposes that an atom can only undergo harmonic isotropic motions around its equilibrium position. For $Q \to 0$, the

ARTICLE IN PRESS

approximation is strictly valid, and it holds up to $\langle u^2 \rangle Q^2 \approx 2$. The MSD can thus be obtained for each temperature by the slope of the semi-logarithmic plot of the incoherent scattering function through

$$\langle u^2 \rangle \approx -6 \frac{\partial \ln S(Q,\omega \approx 0)}{\partial Q^2}. \quad (2)$$

The dynamic structure factor $S(Q, \omega)$ to which QENS experiments give access describes the scattering signal [19], which is a function of the modulus of the momentum transfer Q and of the energy transfer ω, both in units of ħ:

$$S(Q,\omega) = \left[A_0(Q)\delta(\omega) + \sum_i A_i(Q) L_i(\Gamma_i, \omega) + B(Q)\right]. \quad (3)$$

It contains an elastic part, proportional to a delta-function in ω and representing the particles whose motions are not resolved within the instrumental resolution, and a sum over Lorentzian functions L_i, which describe each a different motional contribution included in the QENS part, with a half width half maximum (HWHM) Γ_i. In particular the Γ's contain information about the molecular motions, and can be related to physical quantities, such as diffusion coefficients or residence times, depending on the type of motions involved. A possible inelastic contribution is neglected here. B(Q) accounts for an apparent linear background represented by B(Q) = nQ + m, where n and m are variables accounting for sample (e.g., fast motions outside the spectrometer range) and instrument contributions. Contributions from the empty sample holder were subtracted following standard protocols [19]. For data analysis the structure factor has to be convoluted with the instrumental energy

ARTICLE IN PRESS

resolution R(Q, ω), which can be mimicked by the signal of the elastically and incoherently scattering vanadium:

$$S_{exp}(Q,\omega)=S(Q,\omega)\otimes R(Q,\omega). \quad (4)$$

Application of eq. (4) to fit the data is called the "model-free" procedure, which requests many independent fit parameters and there is no known method to determine exactly how much the sum must be extended. We did a first trial of fits with one, two, and three Lorentzian functions and checked the quality of the fitting. As shown in Figure S1 of the Electronic Supplementary Information (ESI), the spectra were found to be reproduced quite well with two Lorentzians, so that our choice was finally given by:

$$S(Q,\omega) = C(Q)\left\{A_0(Q)\delta(\omega) + \sum_{i=1}^{2} A_i(Q)\frac{\Gamma_i(Q)}{\omega^2+\Gamma_i(Q)^2}\right\} \otimes R(Q,\omega) + B(Q). \quad (5)$$

Here C(Q) is an arbitrary factor permitting to adjust the heights of the scattering curves. The amplitude A_0 is the so-called Elastic incoherent structure factor (EISF) representing the part of particles seen as immobile for high Q values within the instrumental resolution. For the amplitudes A_1 and A_2 it holds that $A_0 + A_1 + A_2 = 1$, so that A_1 or A_2 can be calculated from the other two amplitudes.

The Lorentzian functions give access to parameters of the motions, which can be extracted from their HWHM $\Gamma_i(Q)$. The form of the HWHM as function of Q^2 informs about the type of movements present in the sample. A pure translational diffusion in an unlimited homogeneous medium corresponds to Brownian motion [19] whose characteristics are a linear

ARTICLE IN PRESS

behavior of the HWHM in Q^2. The dynamic structure factor reads in this case:

$$S_T(Q,\omega) = \frac{1}{\pi} \frac{D_T Q^2}{\omega^2 + (D_T Q^2)^2}, \quad (6)$$

where D_T represents the translational diffusion coefficient. This relation usually does not hold in the crowded medium of a macromolecule and has to be generalized to a motion called translational jump-diffusion [30] where the HWHM tends to an asymptotic limit at higher Q values. It describes a situation where the atoms perform oscillatory motions around their equilibrium positions for a time τ_0. After that they diffuse for a time τ_1 by continuous diffusion and these processes are then repeated. The dynamic structure factor can be described by a single Lorentzian with the HWHM Γ_{JD} as

$$\Gamma_{JD} = \frac{D_T Q^2}{1 + D_T Q^2 \tau_0}. \quad (7)$$

At small Q-values, eq. (7) reduces to Brownian's law, and at large Q-values the HWHM tends to the asymptotic value $\Gamma_\infty = 1/\tau_0$, where τ_0 is called the average residence time. In the limit where the HWHM does no longer depend on Q, the motions correspond to rotational diffusion within a confined space [31] and the correlation time of atomic motions τ_i, which is the inverse of Γ_i, can be calculated [32]. In that case, the $A_0(Q)$ can be evaluated analytically [31]:

$$A_0(Q) = \left[\frac{3j_1(Qa)}{Qa}\right]^2, \quad (8)$$

ARTICLE IN PRESS

ARTICLE IN PRESS

where $j_1(x) = \frac{\sin x}{x^2} - \frac{\cos x}{x}$ is a first order spherical Bessel function and a is the radius of a sphere within which atoms can move. Bellisent-Funel et al. [33] expanded this model by an immobile fraction p, whose motions are not resolved by the current energy resolution. The corresponding equation reads:

$$A_0(Q) = p + (1 - p)\left[\frac{3j_1(Qa)}{Qa}\right]^2. \quad (9)$$

RESULTS

IN13. EINS data of fully hydrated PS533 and FB122 samples were taken on IN13 and analysed according to eq. (2) to get the MSD as function of temperature (see Figure 3). The MSD are in very good agreement with our previous results from IN13 [21] (see Figure 6 therein), although absolute values are slightly different due to small variations in hydration level. As in the previous publication, we did the analysis for two different Q-ranges: 0.5–1.67 $Å^{-1}$ (called "low Q" hereafter) and 1.4–2.02 $Å^{-1}$ (called "high Q" hereafter), with $Q = (2\pi)/d$ and d representing the spatial dimension in Å. The differentiation between the two Q-ranges might appear arbitrary, as the PS533 curve at low Q values could have been fitted as well with a straight line. However, for the sake of comparison with earlier data and to show the reproducibility, we maintained here the same approach as in ref. [21]. The DPA-less FB122 is again more mobile than PS533 whatever the Q-range and a change in slope around 302 K is also only visible for PS533 in the low Q-range, probably due to germination. For all other samples and Q-ranges, the MSD change very

ARTICLE IN PRESS

little and almost stay within error bars indicating a high resistance against temperature changes.

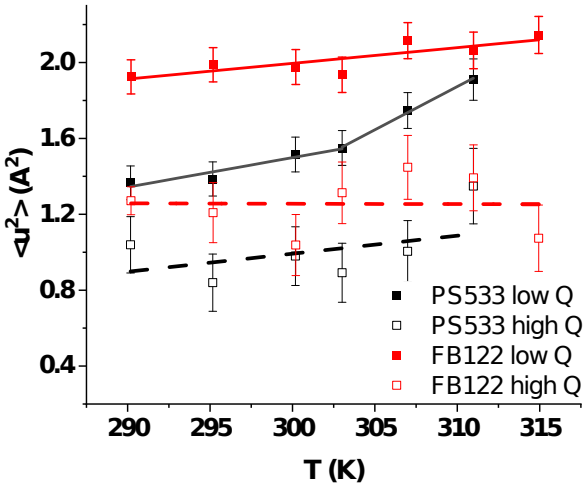

Figure 3: Mean square displacements $\langle u^2 \rangle$ as function of temperature for the wild-type (PS533) and DPA-less form (FB122) of *Bacillus subtilis* measured on IN13.

IN16B. All QENS data sets of IN16B were analysed with the model given by eq. (5). The samples were measured between 290 and 315 K in steps of 5 K, but as the variations in temperature were very weak, we summed up two data sets taken at the nearest temperatures and present them here for the average values of 293, 303 and 313 K.

ARTICLE IN PRESS

ARTICLE IN PRESS

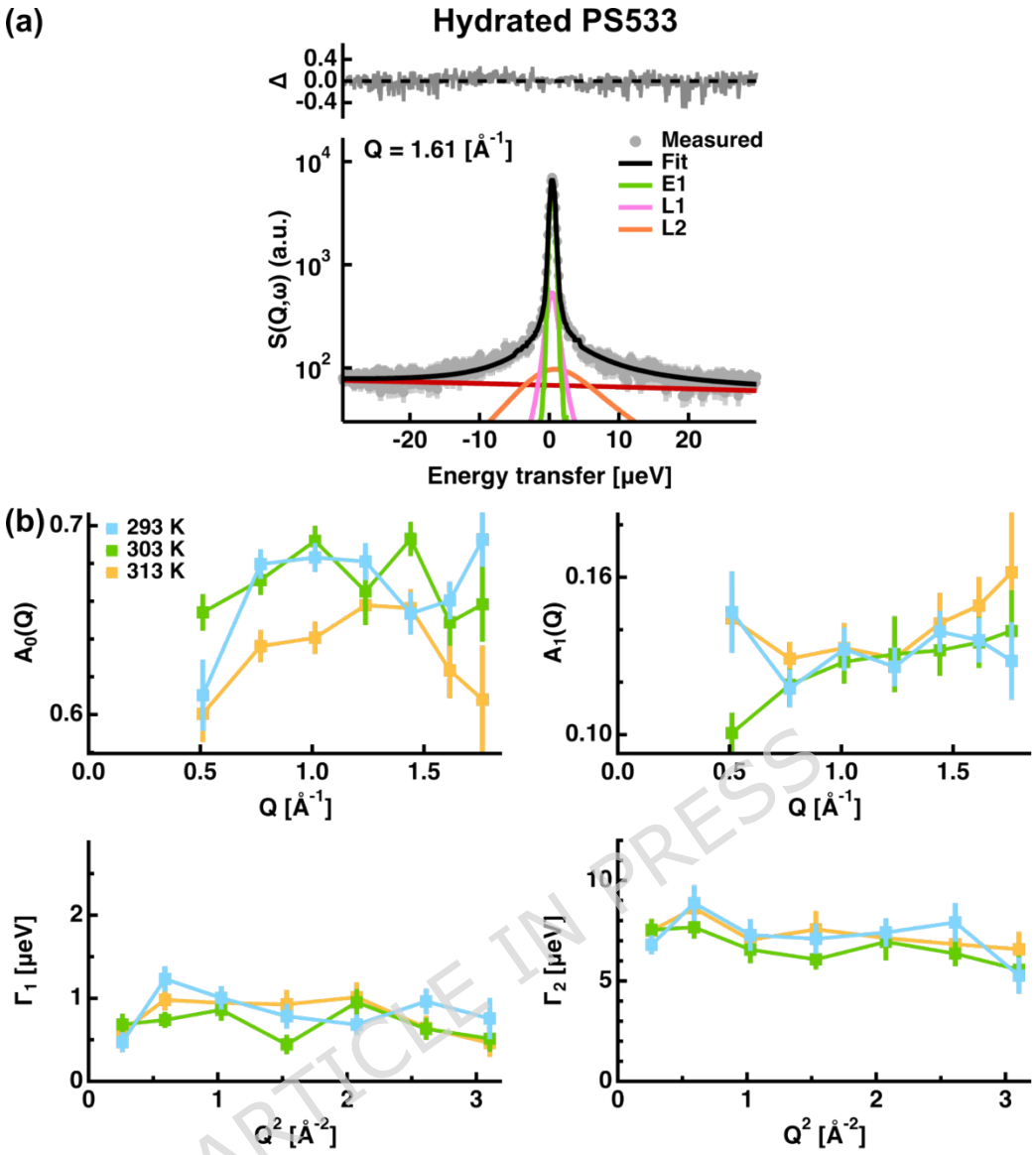

Figure 4. An example of the QENS spectra analysis of bacterial spores taken on IN16B. (a): A fitting example showing hydrated PS533 taken at 313 K and Q = 1.61 Å^{-1}. The measured values are denoted by grey filled circles. The green, magenta, and orange lines represent the elastic component, the narrower Lorentzian L_1, and the wider Lorentzian L_2, respectively. The black line denotes the total fit and the background is shown by a red line. The upper panel describes Δ to show the quality of the fitting (for its definition, refer to the main text). (b): Q-dependence of the amplitudes $A_0(Q)$ and $A_1(Q)$ and Q^2-dependence of the HWHM of the Lorentzians (Γ_1 and Γ_2) at different temperatures. The values at 293 K, 303 K, and 313 K are shown by cyan, green, and yellow lines, respectively.

ARTICLE IN PRESS

Figure 4a shows a fit example for hydrated PS533 at Q = 1.6 Å^{-1}. The quality of the fitting was evaluated by the figure of merit (FOM) at $Q = Q_i$, which is defined by

$$FOM = \frac{1}{N_\omega}\sum_j \Delta_j = \frac{1}{N_\omega}\sum_j \frac{|S_{exp}(Q_i,\omega_j) - S_{sim}(Q_i,\omega_j)|}{S_{exp}(Q_i,\omega_j)}, \quad (10)$$

where $S_{exp}(Q_i,\omega_j)$ and $S_{sim}(Q_i,\omega_j)$ are the measured and the fitted dynamic structure factors at $Q = Q_i$ and $\omega = \omega_i$, respectively. N_ω is the number of data points along the ω direction. The FOM value of the fitting shown in Figure 4a is 0.092. Figure 4b shows the extracted fit parameters for the three temperatures of the same sample. What catches the eye is that all amplitudes A_i depend only little on the temperature and were almost constant in Q, meaning that no differences are seen for small or large movements. We further obtained the HWHM Γ_i for the two motional contributions as function of Q^2. Although they differ by almost one order of magnitude indicating two clearly distinct motions, their behavior is almost constant in Q^2 pointing towards rotational diffusive motions.

Fitting examples and the fit results of all the samples including the hydrated PS533 presented above are summarized in Figures S2 and S3 of the ESI, respectively, and the obtained dynamical parameters are tabulated in Table 1.

Table 1: Summary of the dynamical parameters extracted from the IN16B data. The fits were error-weighted, the numbers in brackets denote one sigma confidence bounds from these fits. The correlation times τ_1^{IN16B} and τ_2^{IN16B} were calculated as the inverse of Γ_1 and Γ_2.

ARTICLE IN PRESS

T(K)	Hydrated PS533 293 303 313			Hydrated FB122 293 303 313			Hydrated and decoated PS533 293 303 313			Hydrated and decoated FB122 293 303 313		
A_0	0.673 (0.004)	0.674 (0.004)	0.640 (0.004)	0.562 (0.005)	0.560 (0.005)	0.558 (0.005)	0.64 (0.02)	0.61 (0.02)	0.62 (0.03)	0.543 (0.005)	0.552 (0.005)	0.539 (0.009)
τ_1^{IN16B} (ps)	813 (55)	966 (68)	833 (60)	944 (84)	859 (70)	739 (53)	2157 (364)	2414 (554)	2291 (697) 107 (9)	598 (54)	710 (74)	836 (120)
τ_2^{IN16B} (ps)	92 (4)	98 (3)	90 (4)	103 (5)	101 (5)	101 (3)	106 (7)	112 (8)		91 (6)	98 (6)	100 (8)

T(K)	Dried PS533 293 303 313			Dried FB122 293 303 313		
A_0	0.837 (0.006)	0.840 (0.005)	0.818 (0.005)	0.790 (0.007)	0.76 (0.01)	0.75 (0.01)
τ_1^{IN16B} (ps)	2094 (384)	1319 (224)	1347 (265)	1734 (211)	1872 (248)	2362 (291)
τ_2^{IN16B} (ps)	138 (10)	124 (10)	217 (18)	104 (7)	110 (6)	98 (6)

ARTICLE IN PRESS

IN6. On IN6, we measured less samples due to beam time constrains. We had originally PS533 and FB122 in their hydrated form and at 75% rh, but the fully hydrated sample of FB122 lost a significant amount of water during the experiment (probably due to a manufactory defect of the sample holder), so that we could not take this data into account. The other data were analysed with the same model as before, but all temperatures were treated separately.

Figure 5 shows the fit results for dried PS533 (Figure 5a and c) and dried FB122 (Figure 5b and d). As clearly seen, the fit quality is quite good. We used eq. (9) to fit the EISF. The amplitudes $A_i(Q)$ are again only very little

ARTICLE IN PRESS

dependent on temperature showing the high resistance of the samples against such variations. The EISF $A_0(Q)$ was found to decrease to ~0.6 at higher Q, suggesting that about 60 % of hydrogen atoms are seen as immobile for both samples though the asymptotic value of FB122 is smaller than that of PS533 in agreement with the higher MSD found on IN13 for this sample. The widths of the two Lorentzians Γ_1 and Γ_2 showed a more or less Q-independent behavior, indicative of a rotational diffusion at different time scales from each other. We also calculated the correlation times of atomic motions τ_i^{IN6} as inverse of the Γ_i. The resultant dynamical parameters are summarized in Table 2.

ARTICLE IN PRESS

ARTICLE IN PRESS

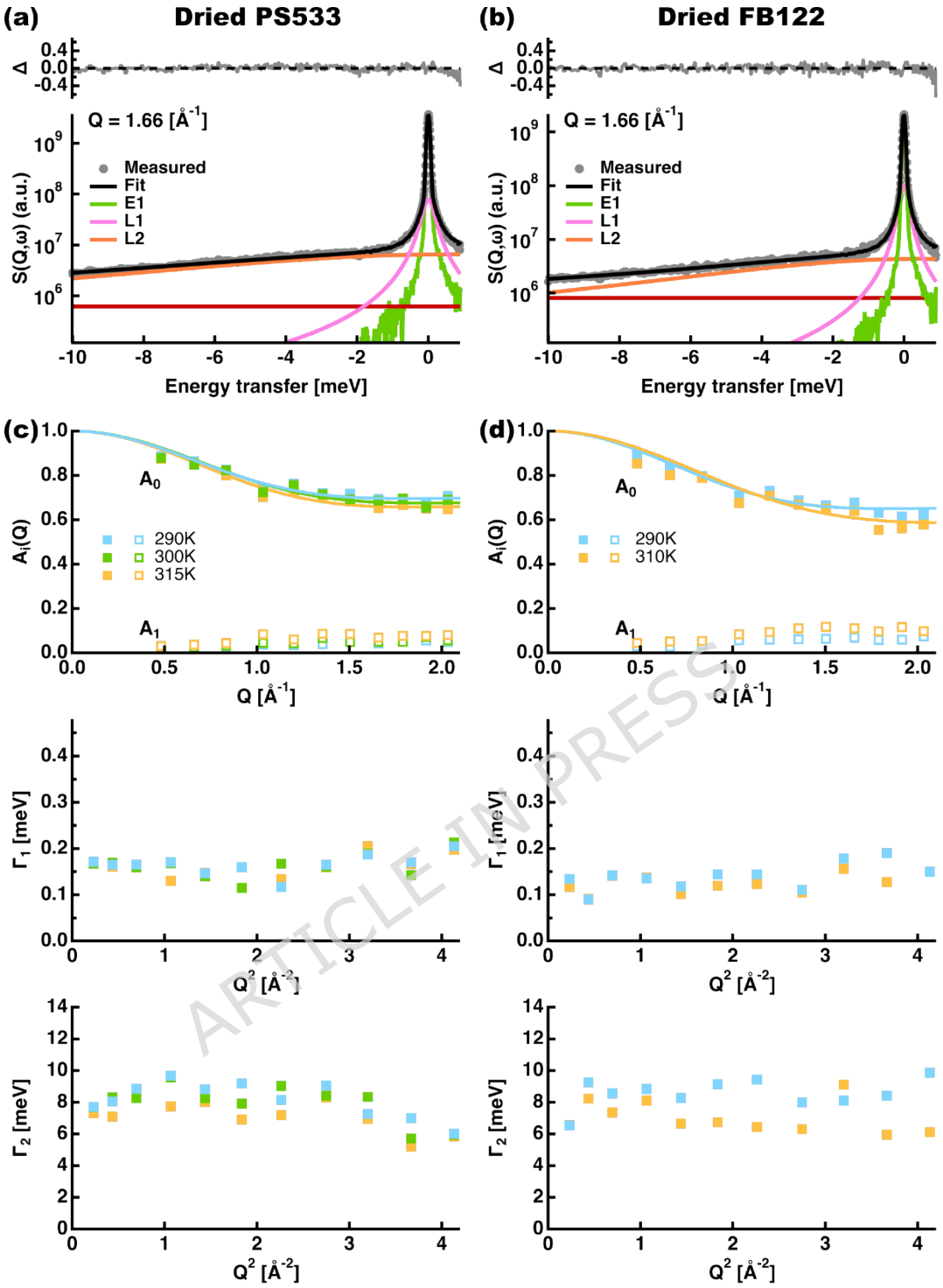

Figure 5. Fitting results of the QENS spectra of dried bacterial spores taken on IN6. (a and b): Fitting examples of the spectra of the dried PS533 at 315 K (a) and the dried FB122 at 310K (b) at Q = 1.66 Å^{-1}, respectively. The FOM values are 0.044 and 0.054 for (a) and (b), respectively. The color scheme is the same as in Fig. 3 (a). (c and d): From the top to the bottom, Q-dependences of the amplitudes $A_0(Q)$ and $A_1(Q)$ and Q^2-dependences of the HWHM of Lorentzians (Γ_1 and Γ_2) of the dried PS533 (c) and the dried FB122 (d) at all the temperatures measured. $A_0(Q)$ and $A_1(Q)$ are extracted by the fitting of eq. (5), denoted by filled and open

ARTICLE IN PRESS

squares, respectively, and the lines correspond to fitting of eq. (9) to the $A_0(Q)$ data.

Table 2. The dynamical parameters obtained from the spectra of dried PS533 and FB122 on IN6 according to eq. (9). The correlation times τ_1^{IN6} and τ_2^{IN6} were calculated as the inverse of Γ_1 and Γ_2. Errors associated with the fitting were not shown because they were too small (on the order of 10^{-10}). Data errors were used as weights in the fitting procedure.

	Dried PS533			Dried FB122	
T(K)	290	300	315	290	310
p	0.70	0.67	0.66	0.65	0.59
a [Å]	2.50	2.36	2.42	2.43	2.07
τ_1^{IN6} (ps)	4.24	4.44	4.51	4.8	5.4
τ_2^{IN6} (ps)	0.09	0.10	0.10	0.08	0.1

Figure 6 shows the fit results for hydrated PS533 at Q = 1.66 $Å^{-1}$, the EISF $A_0(Q)$ and the HWHM Γ_i as a function of Q^2. The fit quality is again excellent, but the fitting results in qualitatively different motional contributions. The amplitudes $A_0(Q)$, which are equal to 1 for Q → 0 by definition (see eq. (9)), increase strongly at low Q and tend to a value around 0.2 at high Q pointing toward 20 % of particles seen as immobile for all temperatures. The amplitudes $A_1(Q)$ are generally smaller and do not depend strongly on temperature. The Lorentzians' widths present different behaviors: Γ_1 is increasing and tending towards a constant value for high Q, a typical characteristic of jump-diffusional behavior [30] (see eq. (7)). Γ_2 is again constant in Q corresponding to rotational diffusion. The fitting results are summarized in Table 3.

ARTICLE IN PRESS

ARTICLE IN PRESS

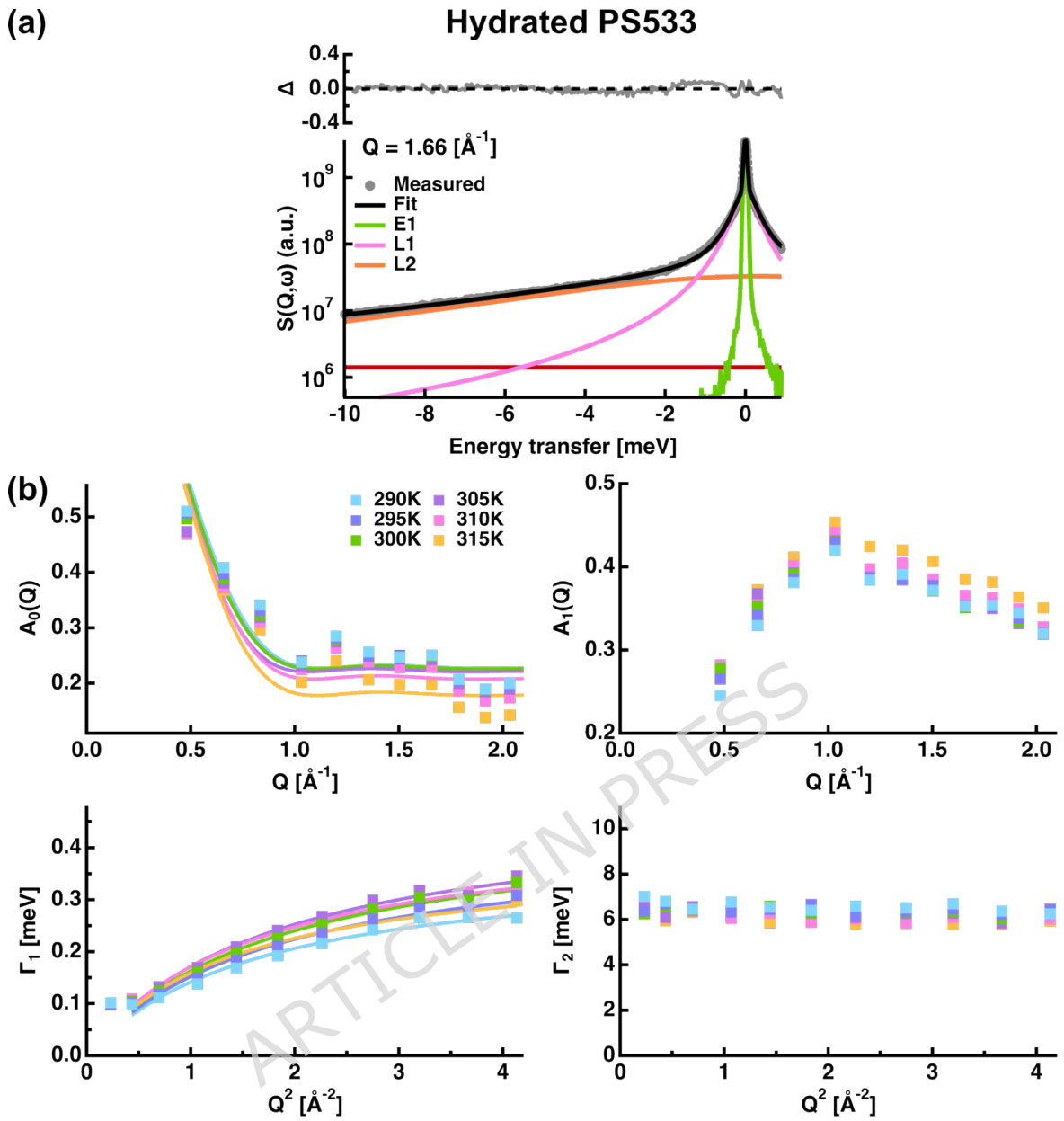

Figure 6. An example of the analysis of the QENS spectra of bacterial spores taken on IN6. (a): A fitting example of the spectra of the hydrated PS533 taken at 310 K and Q = 1.61 Å^{-1}. The color scheme is the same as in Fig. 3 (a). The FOM value is 0.030. (b): Q-dependences of the amplitudes $A_0(Q)$ and $A_1(Q)$ and Q^2-dependences of the HWHM of Lorentzians (Γ_1 and Γ_2) at every 5 K from 290 K to 315 K. $A_0(Q)$ and $A_1(Q)$ are extracted by the fitting of eq. (5), denoted by filled and open squares, respectively, and the lines correspond to fitting of eq. (9) to the $A_0(Q)$ data. Γ_1 was fitted with eq. (7).

ARTICLE IN PRESS

Table 3. The dynamical parameters obtained from the spectra of hydrated PS533 on IN6 based on eqs. (7) and (9). Errors associated with the fitting were smaller than 10^{-4} due to the good statistics of the measurements and data errors used as weights for the fitting.

T(K)	290	295	300	305	310	315
p	0.227	0.226	0.226	0.221	0.208	0.178
a (Å)	4.020	4.098	4.093	4.233	4.136	4.069
D_T (10^{-5}	3.40	3.56	3.78	4.00	4.15	4.05
cm^2/s)	1.75	1.56	1.44	1.38	1.48	1.7
τ_T^{IN6} (ps)	0.101	0.103	0.104	0.106	0.109	0.111
τ_2^{IN6} (ps)						

Whereas the types of the atomic motions are characterized by the fitting, precaution needs to be taken for interpreting the data because the spectra of hydrated PS533 taken on IN6 contain non-negligible contributions from water molecules in the sample in addition to macromolecules unlike the spectra taken on IN16B. The various motional contributions could now be possibly attributed to molecular groups within the sample. However, our specific interest in this study was to characterize the water motions inside the spores, whose dynamics are scarcely known and highly debated. For this purpose, we tried to separate the main contributions from the spores and the water and first estimated the macromolecular contributions knowing that neutron scattering only sees the entire spores and cannot distinguish between various parts as the cortex, coat or core. Spores are known to be mainly composed by about 50 % of proteins, 3 % of lipids, 29 % of peptidoglycan, 10% of DPA, 5 % of DNA and 3 % ions [34,35]. We further assume that DNA is big and their movements too slow to be resolved here

ARTICLE IN PRESS

[36]. Our strategy to extract information on water motions from the QENS spectra of hydrated PS533 was thus the following:

1. Simulating QENS spectra of the proteins, lipids and sugars using literature values and taking into account the relative contributions.
2. Subtracting these simulated spectra from the spectra of PS533.
3. The resultant spectrum must then arise from water dynamics in the spore.

We had at our disposal typical spectra of a protein collected on IN6, the hydrated CFP protein studied at 310 K [37]. We used the spectra of phospholipid bilayers from 1,2-dimyristoyl-*sn*-glycero-3-phosphocholine (DMPC) studied on IN6 at 311 K [38] and of glucose taken on IN6 at 300K (unpublished data kindly provided by Profs. A. Paciaroni and S. Capaccioli). Assuming in the concrete case a spore chemical composition (by weight) of 50% proteins, 3% of lipids and 29% of sugar, we were able to fit the PS533 spectra at 310 K with these contributions (Figure 7a) and could thus model the spectrum of water contained in the spores (in blue in the Figure 7a), which was then fitted again using an elastic part, two Lorentzian curves and a background (Figure 7b).

ARTICLE IN PRESS

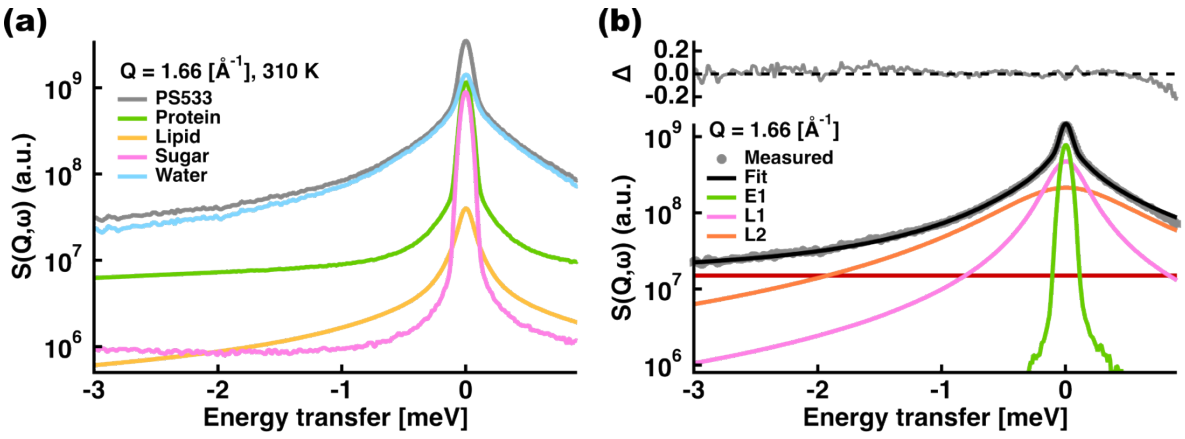

ARTICLE IN PRESS

Figure 7. Extraction of the spectra of water contained in the hydrated PS533 taken on IN6. The spectra at Q = 1.66 Å^{-1} and 310 K are shown. (a): The grey line shows the spectra of the hydrated PS533. The green, yellow, magenta lines denote the simulated spectra of proteins, lipids, and sugar, respectively (for details, please refer to the main text). The pale blue line is the resultant spectrum of water in the spores. (b): A fitting example of the spectrum of water. The green, magenta, and orange lines show the elastic component, the narrower Lorentzian L1 and the broader Lorentzian L2, respectively. The background is denoted by the red line and the total fit is shown by the black line. The FOM value is 0.039.

From these fits we extracted the EISF $A_0(Q)$ (Figure 8a) and the widths of the two Lorentzians, Γ_1 and Γ_2 (Figure 8b and c). The EISF was fitted by the diffusion-inside-the-sphere model [31]. The HWHM of the two Lorentzians could be fitted by the jump-diffusion model [30]. We stopped the fit of Γ_2 below 1 Å^{-2}, because the width increases again pointing toward confinement effects. The fit parameters obtained are summarized in Table 4.

ARTICLE IN PRESS

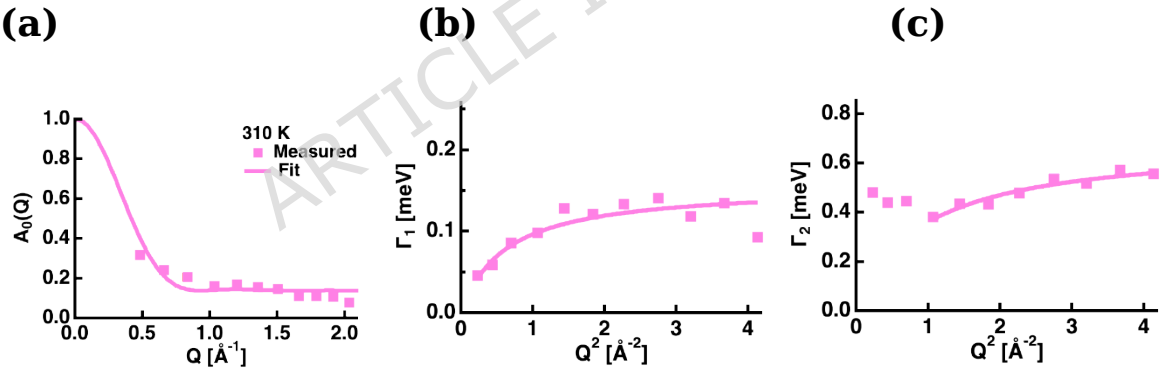

Figure 8. Results of the analysis of the spectra of water in the hydrated PS533. Q- dependence of the amplitude $A_0(Q)$ and Q^2-dependences of the HWHMs of the two Lorentzians (Γ_1 and Γ_2) are shown in (a), (b), and (c), respectively. $A_0(Q)$ was extracted by the fitting of eq. (5) and the line corresponds to fitting of eq. (9) to the $A_0(Q)$ data. Γ_1 and Γ_2 was fitted with eq. (7).

Table 4. The dynamical parameters obtained from the spectra of water in the hydrated PS533 at 310 K according to eqs. (7) and (9). Errors associated with the fitting could not be evaluated because the extraction of the spectra of water includes the use of simulated (theoretical) spectra.

ARTICLE IN PRESS

P	a [Å]	D_1 [cm^2/s]	τ_1^{IN6} [ps]	D_2 [cm^2/s]	τ_2^{IN6} [ps]
0.14	4.83	$3.81\ 10^{-5}$	4.25	$1.15\ 10^{-4}$	0.97

DISCUSSION

Within all these measurements, we got a panoply of results requiring interpretation. One should note that neutron scattering gives only access on averages over all possible motions of H-atoms. Principally, one could apply the technique of contrast variation by exchanging parts of the Hydrogen atoms against Deuterium, the isotope with a much smaller incoherent cross section, but it is not possible in case of spores. This was also the reason why we tried to access water dynamics in the way described above.

Another general remark is in order here: the instruments IN6 and IN16B dispose of very different energy resolutions, namely, 90 and 0.75 μeV HWHM in the chosen configurations corresponding to time windows of about 10 ps and 1 ns. The combination of both permits to sample various movements like a motion filter [39]. However, not surprisingly, the correlation times of atomic motions τ_1 and τ_2 somehow also scale with the resolution even if it is not linear. In this sense, we can compare these quantities among different samples measured on the same instrument, but it does not make sense to compare them with values obtained on another instrument.

We suppose that we mainly observe the motions of the proteome on IN16B, because it represents the most abundant dry weight cellular

ARTICLE IN PRESS

composition. Peptidoglycans and DNA form long chains and their global motions correspond to another time scale. In the inner membrane, a high degree of lipid immobilization was reported [5] so that lipids will also be less important. These facts are mirrored in figure 7a, where in addition to water the proteins have the highest contribution. The contribution of the peptidoglycans and DNA stays mainly within the elastic peak moving only little and the lipids are represented by a Lorentzian curve with a small absolute value although they have a broader widening corresponding to small motions.

Dynamical differences between PS533 and FB122

The measurements on IN16B allow to observe the dynamics of bio-macromolecules in the spores (see Table 1), because the energy resolution of IN16B (~0.75 μeV) is extremely high such that the scattering contribution from water molecules appears mainly as an apparent flat background. The dynamics of the center-of-mass motion of the entire spores with or without DPA are characterized by the IN16B data of the hydrated PS533 and FB122 samples. The EISF A_0, which appears almost constant as function of Q, represents particles seen as immobile. It is systematically slightly lower for the decoated particles. The coat proteins are indeed organized in dense, cross-linked layers [40,41] and are expected to be much less mobile. Strikingly, the EISF is lower for FB122 than for PS533, because crowding in the core is reduced in the mutant giving more space for motions in the latter case. Generally speaking, the A_0 depend only very little on temperature (nota bene: we increased a lot the scale on

ARTICLE IN PRESS

the y-axis) and decrease only slightly at 313 K translating more dynamics at higher temperature, as expected. However, this fact indicates a high stability of the spores against temperature increase.

The motions observed on IN16B correspond to two types of rotational diffusion within the proteome. It is very unusual to find two rotational diffusive motions, but rather a translational or jump-diffusive motion together with another rotational diffusion. This is a first indication for a drastic slow-down of the molecular dynamics, strong effects due to confinement and eventually a disturbance of the water network with increased mobility in the hydration shell despite a hydration of h = 0.6 comparable or even higher than hydrated powders used for neutron scattering experiments [42]. Generally speaking, the correlation times τ_1^{IN16B} and τ_2^{IN16B} are long indicating that the spore proteins are even though not rotationally immobilized, at least significantly slowed down as it can be found typically in protein powders hydrated at around h = 0.4 [42]. The correlation times seem almost independent on temperature within error bars referring to a protective effect of crowding. τ_1^{IN16B} is much higher for decoated PS533. The reason for that is not clear. τ_2^{IN16B}, representing the fast motions likely related to protein side chains and small molecular subgroups, does neither depend on temperature nor on the sample type, as local motions are much less affected than slower global motions within a cellular environment [43]. These findings are consistent with our previous results [21].

Dried PS533 and FB122 samples have, as expected, globally higher immobile fractions of atoms, but they are slightly lower for the DPA-less

ARTICLE IN PRESS

spores FB122. The correlation times τ_1^{IN16B} are affected with high error bars and thus not very meaningful, unless in the sense that they are higher than for the hydrated samples, what holds also for τ_2^{IN16B}.

The measurements on IN6 of the same samples permit to observe atomic motions at a much shorter time scale of about 10 ps and can therefore be preferentially attributed to water molecule motions and small motions of molecular subgroups at the proteins' surfaces and in close interaction with water. For the dried samples (see Table 2), the immobile fraction p decreases with increasing temperature, as expected, and is slightly lower for the DPA-less FB122. The correlation time arising from slower motions, τ_1^{IN6}, is larger for FB122 and the correlation time from faster motions, τ_2^{IN6}, is the same between the two samples. This indicates that in the DPA-less spores, some atomic motions are enhanced compared with the wild-type, but these motions are slow, resulting in a larger τ_1^{IN6} than for the wild-type. Both the IN16B and IN6 data thus suggest that the biomolecules in the DPA-less spores show higher mobility irrespective of the existence of water molecules. The contribution of the slower motions is also in agreement with the finding that DPA exists as an amorphous aggregate [44,45].

As explained earlier, the data of hydrated FB122 was not usable, but we fitted the curves of hydrated PS533 as function of temperature (see Table 3). Here, the immobile fraction was much lower and decreased also with temperature, as expected for a more and more mobile sample. The radius *a* was almost independent of temperature at around 4 Å pointing toward confinement which is not temperature-dependent. Two dynamical

ARTICLE IN PRESS

populations could be distinguished: the slower one corresponding to jump-diffusion with a translational diffusion coefficient D_T higher than that of bulk water [46] and a residence time τ_T^{IN6} around 1.5 ps. As stated previously by Trapp et al. [47], these values could be considered as an effective diffusion coefficient depending on the current energy resolution as the time window could not be sufficient to follow the complete motion and thus appear too high. The second faster movement corresponds to rotational diffusion and one gets values of τ_2^{IN6} very similar to those of the dried samples. These findings suggest that there might indeed be a part of the proteome in close interaction with water and showing similar motional characteristics, and a second one with a considerable but very localized dynamics.

ARTICLE IN PRESS

Dynamical behavior of water molecules in the spores

In general, liquid water does not generate an elastic peak in the QENS spectra as no molecules should be immobile. However, a remnant elastic peak was observed here as shown in Figure 7b, resulting in the immobile fraction of p = 0.14 (Table 4). It is thus possible that a small amount of water molecules is strongly bound to macromolecules in the spores, but a residual scattering contribution from macromolecules in the spectra of water can also not be ruled out. Stadler et al. [48] also found an immobile water fraction in red blood cells around 10 %.

We fit best our data using two Lorentzian curves, what means that besides the “immobile” water, we see two other populations representing water

ARTICLE IN PRESS

which is more or less bound to the surface of the proteins and other molecules in their environment.

The radius of a sphere, *a*, of water motions was found to be larger than that of other protein atoms measured on the same spectrometer [37,42], but very similar to those obtained for the hydrated PS533 (see Table 4). This implies that water molecules are quite mobile here, but that they are confined within a cage formed by a macromolecular network. Regarding the diffusion coefficients of the water molecules, D_2 was found to be larger than that of bulk water at 310 K and D_1 was close to it [46]. Remarkably, the value found for D_1 was again very similar to that extracted for hydrated PS533 showing that a strong interaction might exist between one water population and the surface of the proteins [49]. On the contrary, D_2 was even bigger than D_1. Even though a certain overestimation due to resolution effects cannot be excluded, it clearly points toward highly mobile water at a localized scale. Indeed, some molecules or solutes can break the structure of the hydrogen-bonded network of neighboring water molecules and have a negative hydration effect making the water molecules hypermobile as compared to those in the bulk phase [50 51].

The residence times were similar (τ_2^{IN6}) or slightly larger than in bulk water [52]. It is thus unlikely that in the spore, there exist water molecules whose motions are highly restricted as seen in typical hydration water around proteins or in cells [53,54]. Combined with the value of the immobile fraction, water molecules inside and outside of the spore appear to show enhanced dynamics compared with typical hydration water. Since molecules with higher mobility easily respond to changes in the surrounding conditions

ARTICLE IN PRESS

such as heat, it is likely that biomolecules moving slowly in the presence of DPA molecules in the core contribute to the heat resistance of the spore.

Conclusions

In the present study, we investigated bacterial spores in their wild-type form (PS533) and a mutant lacking DPA (FB122). To obtain an as complete description as possible, we used incoherent neutron scattering on two spectrometers with different resolutions representing time windows of about 1 ns and 1 ps. We measured hydrated and dried samples on both instruments as well as decoated ones on IN16B. The data permitted to see that for all samples and both resolutions, we were able to fit the data with two Lorentzian functions representative of two distinct motions. Comparison with values in the literature permitted a tentative attribution of the motions to certain molecular species, however such approach is not a direct proof. This method is commonly used and based on van Hove's classical pair correlation function [55] and proofed to be successful in describing molecular motions within complex samples [16,56]. However, to avoid over-fitting, eq. (3) needs to be truncated to a small number of Lorentzian functions. In addition, the motions as internal molecular vibrations, molecular reorientations or centre-of-mass translations are observed at well separated time scales, so that a simple sum instead of convolutions of Lorentzian functions can be justified [57]. Such combination of approximations leads necessarily to uncertainties in the data analysis which should not be undervalued. Nonetheless, the

ARTICLE IN PRESS

results presented here are in very reasonable agreement to those obtained by similar studies [46,48] and are thus used for first conclusions.

DPA-less samples show slightly enhanced water dynamics than the wild-types. Whereas the proteome's motions at a time scale of 1 ns appeared significantly slowed down, probably due to crowding inside the spores, the outcome was opposite at 10 ps, where the movements were comparable or enhanced compared to bulk water. Obviously, slow dynamics of domains or molecules like lipids accompanied by fast localized motions of small molecular subgroups and water molecules seem to be key to maintain the spore in a state which is close enough to the physiological one and permits germination whenever the external conditions allow it. The EISF presented a surprising constant behavior with temperature pointing toward a high stability of the spores likely enabling them in such a way to better thrive with such extreme external conditions.

ARTICLE IN PRESS

Conflict of interest

There are no conflicts to declare.

Data availability

Data are available under https://doi.ill.fr/10.5291/ILL-DATA.8-04-686.

Acknowledgements

The authors wish to thank the Institut Laue Langevin (ILL) for beam time allocation. We are also grateful to Pr Peter Setlow and Pr Barbara Setlow for providing us the mutant strains and for their advices during the experiments.

ARTICLE IN PRESS

This work is a part of the sHpore project funded by “Carnot Qualiment”. This work is also supported by the Bourgogne-Franche-Comté Regional Council and the European Regional Development Fund (FEDER).

References

1 Setlow, P. & Christie, G. New Thoughts on an Old Topic: Secrets of Bacterial Spore Resistance Slowly Being Revealed. *Microbiol Mol Biol Rev* **87**, e0008022 (2023). https://doi.org/10.1128/mmbr.00080-22

2 Leggett, M. J., McDonnell, G., Denyer, S. P., Setlow, P. & Maillard, J. Y. Bacterial spore structures and their protective role in biocide resistance. *J Appl Microbiol* **113**, 485–498 (2012). https://doi.org/10.1111/j.1365-2672.2012.05336.x

3 Bratbak, G. Bacterial Biovolume and Biomass Estimations. *Appl Environ Microbiol.* **49**, 1488–1493 (1985).

4 Setlow, P. Observations on research with spores of Bacillales and Clostridiales species. *J Appl Microbiol* **126**, 348–358 (2019). https://doi.org/10.1111/jam.14067

5 Sunde, E. P., Setlow, P., Hederstedt, L. & Halle, B. The physical state of water in bacterial spores. *Proc Natl Acad Sci U S A* **106**, 19334–19339 (2009). https://doi.org/10.1073/pnas.0908712106

6 Friedline, A. W. *et al.* Water behavior in bacterial spores by deuterium NMR spectroscopy. *J Phys Chem B* **118**, 8945–8955 (2014). https://doi.org/10.1021/jp5025119

7 Kaieda, S., Setlow, B., Setlow, P. & Halle, B. Mobility of core water in Bacillus subtilis spores by 2H NMR. *Biophys J* **105**, 2016–2023 (2013). https://doi.org/10.1016/j.bpj.2013.09.022

8 Leuschner, R. G. & Lillford, P. J. Thermal properties of bacterial spores and biopolymers. *Int J Food Microbiol* **80**, 131–143 (2003). https://doi.org/10.1016/s0168-1605(02)00139-3

9 Paciaroni, A., Cinelli, S. & Onori, G. Effect of the Environment on the Protein Dynamical Transition: A Neutron Scattering Study. *Biophys J* **83**, 1157 – 1164 (2002).

10 Perticaroli, S. *et al.* Description of Hydration Water in Protein (Green Fluorescent Protein) Solution. *J Am Chem Soc* **139**, 1098–1105 (2017). https://doi.org/10.1021/jacs.6b08845

11 Doster, W., Cusack, S. & Petry, W. Dynamical transition of myoglobin revealed by inelastic neutron scattering. *Nature* **337**, 754–756 (1989). https://doi.org/10.1038/337754a0

12 Frauenfelder, H., Parak, F. & Young, R. D. Conformational substates in proteins. *Annu. Rev. Biophys. Biophys. Chem.* **17**, 569 – 572 (1988).

13 Peters, J., Oliva, R., Calio, A., Oger, P. & Winter, R. Effects of Crowding and Cosolutes on Biomolecular Function at Extreme

ARTICLE IN PRESS

Environmental Conditions. *Chem Rev* **123**, 13441–13488 (2023). https://doi.org/10.1021/acs.chemrev.3c00432

14 Ellis, R. J. Macromolecular crowding: an important but neglected aspect of the intracellular environment. *Curr. Opin. Struct. Biol.* **11**, 114–119 (2001).

15 Zimmerman, S. B. & Minton, A. P. Macromolecular crowding: biochemical, biophysical, and physiological consequences. *Annual review of biophysics and biomolecular structure* **22**, 27–65 (1993). https://doi.org/10.1146/annurev.bb.22.060193.000331

16 Grimaldo, M., Roosen-Runge, F., Zhang, F., Schreiber, F. & Seydel, T. Dynamics of proteins in solution. *Quaterly Reviews of Biophysics* **52**, e7 (2019).

17 Zhang, P., Setlow, P. & Li, Y. Characterization of single heat-activated Bacillus spores using laser tweezers Raman spectroscopy. *Opt Express* **17**, 16480–16491 (2009). https://doi.org/10.1364/OE.17.016480

18 Sears, V. F. Neutron scattering lengths and cross sections. *Neutron News* **3**, 26–37 (1992).

19 Bée, M. *Quasielastic Neutron Scattering:Principles and Applications in Solid State Chemistry, Biology and Materials Science*. (Adam Hilger, Philadelphia, 1988).

20 Paidhungat, M., Ragkousi, K. & Setlow, P. Genetic requirements for induction of germination of spores of Bacillus subtilis by Ca(2+)-dipicolinate. *J Bacteriol* **183**, 4886–4893 (2001). https://doi.org/10.1128/JB.183.16.4886-4893.2001

21 Colas de la Noue, A. *et al.* The molecular dynamics of bacterial spore and the role of calcium dipicolinate in core properties at the sub-nanosecond time scale. *Sci Rep* **10**, 8265 (2020). https://doi.org/10.1038/s41598-020-65093-y

22 Paidhungat, M. & Setlow, P. Localization of a germinant receptor protein (GerBA) to the inner membrane of Bacillus subtilis spores. *J Bacteriol* **183**, 3982–3990 (2001). https://doi.org/10.1128/JB.183.13.3982-3990.2001

23 Tehei, M. *et al.* Neutron scattering reveals extremely slow cell water in a Dead Sea organism. *Proc Natl Acad Sci U S A* **104**, 766–771 (2007). https://doi.org/10.1073/pnas.0601639104

24 Natali, F. *et al.* IN13 Backscattering Spectrometer at ILL: Looking for Motions in Biological Macromolecules and Organisms. *Neutron News* **19**, 14–18 (2008). https://doi.org/10.1080/10448630802474083

25 Frick, B., Mamontov, E., van Eijck, L. & Seydel, T. Recent Backscattering Instrument Developments at the ILL and SNS. *Z Phys Chem* **224**, 33–60 (2010). https://doi.org/10.1524/zpch.2010.6091

26 Colas de la Noue, A., Natali, F., Perrier-Cornet, J. M. & Peters, J. (Institut Laue Langevin, DOI: 10.5291/ILL-DATA.8-02-686), 2013).

27 Paalman, H. H. & Pings, C. J. Numerical Evaluation of X-Ray Absorption Factors for Cylindrical Samples and Annular Sample Cells. *J Appl Phys* **33**, 2635–& (1962). https://doi.org/Doi 10.1063/1.1729034

ARTICLE IN PRESS

28 Richard, D., Ferrand, M. & Kearley, G. J. Analysis and visualisation of neutron-scattering data. *Journal of Neutron Research* **4**, 33–39 (1996). https://doi.org/10.1080/10238169608200065

29 Rahman, A., Singwi, K. S. & Sjolander, A. Theory of Slow Neutron Scattering by Liquids .1. *Phys Rev* **126**, 986–996 (1962). https://doi.org/10.1103/PhysRev.126.986

30 Singwi, K. S. & Sjölander, A. Diffusive Motions in Water and Cold Neutron Scattering. *Phys. Rev.* **119**, 863–871 (1960).

31 Volino, F. & Dianoux, A. J. Neutron Incoherent-Scattering Law for Diffusion in a Potential of Spherical-Symmetry - General Formalism and Application to Diffusion inside a Sphere. *Molecular Physics* **41**, 271–279 (1980). https://doi.org/Doi 10.1080/00268978000102761

32 Perez, J., Zanotti, J. M. & Durand, D. Evolution of the internal dynamics of two globular proteins from dry powder to solution. *Biophys J* **77**, 454–469 (1999). https://doi.org/10.1016/S0006-3495(99)76903-1

33 Bellissent-Funel, M.-C., Teixeira, J., Bradley, K. F. & Chen, S. H. Dynamics of hydration water in protein. *J. Phys. I France* **2**, 995–1001 (1992).

34 Walker, H. W., Matches, J. R. & Ayres, J. C. Chemical composition and heat resistance of some aerobic bacterial spores. *Journal of Bacteriology* **82**, 960 – 966 (1961).

35 Warth, A. D., Ohye, D. F. & Murrell, W. G. The composition and structure of bacterial spores. *J Cell Biol* **16**, 579–592 (1963). https://doi.org/10.1083/jcb.16.3.579

36 Beta, I. A., Michalarias, I., Ford, R. C., Li, J. C. & Bellisent-Funel, M. C. Quasi-elastic neutron scattering study of hydrated DNA. *Chemical Physics* **292**, 451 – 454 (2003).

37 Golub, M. *et al.* Dynamics of a family of cyan fluorescent proteins probed by incoherent neutron scattering. *J R Soc Interface* **16**, 20180848 (2019). https://doi.org/10.1098/rsif.2018.0848

38 Cisse, A. *et al.* The dynamical Matryoshka model: 2. Modeling of local lipid dynamics at the sub-nanosecond timescale in phospholipid membranes. *BBA - Biomembranes* **1864**, 183950 (2022). https://doi.org/10.1016/j.bbamem.2022.183950

39 Henzler-Wildman, K. & Kern, D. Dynamic personalities of proteins. *Nature* **450**, 964 – 972 (2007).

40 Henriques, A. O. & Moran, C. P., Jr. Structure and assembly of the bacterial endospore coat. *Methods* **20**, 95–110 (2000). https://doi.org/10.1006/meth.1999.0909

41 Ghosh, S. *et al.* Characterization of spores of Bacillus subtilis that lack most coat layers. *J Bacteriol* **190**, 6741–6748 (2008). https://doi.org/10.1128/JB.00896-08

42 Peters, J. *et al.* Dynamics of human acetylcholinesterase bound to non-covalent and covalent inhibitors shedding light on changes to the water network structure. *Phys Chem Chem Phys* **18**, 12992–13001 (2016). https://doi.org/10.1039/c6cp00280c

ARTICLE IN PRESS

43 Di Bari, D. *et al.* Diffusive Dynamics of Bacterial Proteome as a Proxy of Cell Death. *ACS Cent Sci* **9**, 93–102 (2023). https://doi.org/10.1021/acscentsci.2c01078

44 Ablett, S., Darke, A. H., Lillford, P. J. & Martin, D. R. Glass formation and dormancy in bacterial spores. *International Journal of Food Science and Technology* **34**, 59–69 (1999). https://doi.org/10.1046/j.1365-2621.1999.00240.x

45 Kong, L., Setlow, P. & Li, Y. Q. Analysis of the Raman spectra of Ca(2+)-dipicolinic acid alone and in the bacterial spore core in both aqueous and dehydrated environments. *Analyst* **137**, 3683–3689 (2012). https://doi.org/10.1039/c2an35468c

46 Simpson, J. H. & Carr, H. Y. Diffusion and Nuclear Spin Relaxation in Water. *Phys. Rev.* **111**, 1201 – 1202 (1958).

47 Trapp, M. *et al.* Correlation of the dynamics of native human acetylcholinesterase and its inhibited huperzine A counterpart from sub-picoseconds to nanoseconds. *Journal of the Royal Society Interface* **11** (2014). https://doi.org/10.1098/rsif.2014.0372

48 Stadler, A. M. *et al.* Cytoplasmic water and hydration layer dynamics in human red blood cells. *J Am Chem Soc* **130**, 16852–16853 (2008). https://doi.org/10.1021/ja807691j

49 Gallat, F. X. *et al.* Dynamical coupling of intrinsically disordered proteins and their hydration water: comparison with folded soluble and membrane proteins. *Biophys J* **103**, 129–136 (2012). https://doi.org/10.1016/j.bpj.2012.05.027

50 Kabir, S. R., Yokoyama, K., Mihashi, K., Kodama, T. & Suzuki, M. Hyper-mobile water is induced around actin filaments. *Biophys J* **85**, 3154–3161 (2003). https://doi.org/10.1016/S0006-3495(03)74733-X

51 Matsuo, T. *et al.* Difference in the hydration water mobility around F-actin and myosin subfragment-1 studied by quasielastic neutron scattering. *Biochem Biophys Rep* **6**, 220–225 (2016). https://doi.org/10.1016/j.bbrep.2016.04.013

52 Teixeira, J., Bellissent Funel, M. C., Chen, S. H. & Dianoux, A. J. Experimental-Determination of the Nature of Diffusive Motions of Water-Molecules at Low-Temperatures. *Phys Rev A* **31**, 1913–1917 (1985). https://doi.org/DOI 10.1103/PhysRevA.31.1913

53 Natali, F. *et al.* Anomalous water dynamics in brain: a combined diffusion magnetic resonance imaging and neutron scattering investigation. *J R Soc Interface* **16**, 20190186 (2019). https://doi.org/10.1098/rsif.2019.0186

54 Martinez, N. *et al.* High protein flexibility and reduced hydration water dynamics are key pressure adaptive strategies in prokaryotes. *Sci Rep* **6**, 32816 (2016). https://doi.org/10.1038/srep32816

55 Van Hove, L. Correlations in Space and Time and Born Approximation Scattering in Systems of Interacting Particles. *Phys. Rev.* **95**, 249 – 262 (1954). https://doi.org/10.1103/PhysRev.95.249

56 Gabel, F. Protein dynamics in solution and powder measured by incoherent elastic neutron scattering: the influence of Q-range and

ARTICLE IN PRESS

energy resolution. *Eur Biophys J* **34**, 1–12 (2005). https://doi.org/10.1007/s00249-004-0433-0

57 Bée, M. Application de la diffusion inélastique aux systèmes désordonnés. *J. Phys. IV France* **111**, 259 – 296 (2003).

ARTICLE IN PRESS